Multiple forms of copper(II) co-ordination occur throughout the disordered N-terminal region of the prion protein at pH 7.4

Mark A Wells, Clare Jelinska, Laszlo Lp Hosszu, C Jeremy Craven, Anthony R Clarke, John Collinge, Jonathan P Waltho, Graham S Jackson

Biochemical Journal Immediate Publication. Published on 22 Aug 2006 as manuscript BJ20060721

Multiple forms of copper (II) coordination occur throughout the disordered N-terminal region of the prion protein at pH 7.4

Mark A. Wells *†, Clare Jelinska *, Laszlo L. P. Hosszu*†, C. Jeremy Craven*, Anthony R. Clarke†, John Collinge†, Jonathan P. Waltho* and Graham S. Jackson†

* Krebs Institute for Biomolecular Research, Department of Molecular Biology and Biotechnology, University of Sheffield, Sheffield, S10 2TN, UK

† MRC Prion Unit, Department of Neurodegenerative Disease, Institute of Neurology, University College London, Queen Square, London, WC1N 3BG, UK

Corresponding author: Dr Graham S. Jackson
Tel : +44 (0)207 676 2190
Fax : +44 (0)207 676 2180
E-mail: g.s.jackson@prion.ucl.ac.uk

Page heading: Multiple modes of copper binding in the prion protein

Biochemical Journal Immediate Publication. Published on 22 Aug 2006 as manuscript BJ20060721

Synopsis:

Although the physiological function of the prion protein remains unknown, *in vitro* experiments suggest that the protein may bind copper (II) ions and play a role in copper transport or homeostasis *in vivo*. The unstructured N-terminal region of the prion protein has been shown to bind up to six copper (II) ions, with each of these ions coordinated by a single histidine imidazole and nearby backbone amide nitrogen atoms. Individually these sites have micromolar affinities, which is weaker than would be expected of a true cuproprotein. Here we show that with sub-saturating levels of copper different forms of coordination will occur, which have higher affinity. We have investigated the copper binding properties of two peptides representing the known copper binding regions of the prion protein; residues 57-91, which contains four tandem repeats of the octapeptide GGGWGQPH, and residues 91-115. Using equilibrium dialysis and spectroscopic methods we unambiguously demonstrate that the mode of copper coordination in both of these peptides depends on the number of copper ions bound and that at low copper occupancy, copper ions are coordinated with sub micromolar affinity by multiple histidine imidazole groups. At pH 7.4, three different modes of copper coordination are accessible within the octapeptide repeats and two within the peptide comprising residues 91-115. The highest affinity copper (II) binding modes cause self-association of both peptides, suggesting a role for copper (II) in controlling prion protein self-association *in vivo*.

Keywords: PrP, peptides, copper (II), equilibrium dialysis, self-association.

Biochemical Journal Immediate Publication. Published on 22 Aug 2006 as manuscript BJ20060721

Introduction

Prion diseases are a group of transmissible, neurodegenerative disorders, found in both humans and animals, which have become the focus of intense scientific interest because of their apparently unique underlying biology [1]. The 'protein only' hypothesis is now widely accepted and proposes that the causative agent of these diseases is largely, if not exclusively, composed of an abnormal conformer of a host encoded protein known as the prion protein, PrP, and is devoid of nucleic acid [2, 3]. Mature human PrP is a 209 residue polypeptide with a C-terminal glycosylphosphatidylinositol anchor and two glycosylation sites, that comprises a folded C-terminal domain and a flexibly disordered N-terminal region [4-6]. Although much is now known about the disease causing properties of the prion protein, the physiological function of the protein remains an enigma. PrP is expressed in most tissues in adults but the highest levels of expression occur in the central nervous system and the immune system [7, 8]. Transgenic mice in which the *Prnp* gene has been disrupted and hence PrP^C expression is ablated display no developmental or behavioural phenotype [9], although more detailed studies have described electrophysiological abnormalities [10] and alterations in sleep and circadian rhythms [11].

In vitro experiments have revealed that the prion protein specifically binds copper (II) [12-15] and this had led to the proposal that PrP may function as a cuproprotein *in vivo.* However, the evidence for this assertion is limited; mice that do not express PrP have been reported to have reduced levels of copper (II) in membrane fractions from the brain [16] although this result could not be replicated by other investigators [17]. Cultured cells induced to express PrP have been shown to have a higher copper binding capacity than uninduced cells [18]. Copper (II) has also been reported to cause internalisation of PrP but the concentrations required to cause this effect are vastly above measured physiological levels [18, 19].

A clear understanding of the copper (II) binding properties of the prion protein *in vitro* is thus essential in order to critically evaluate proposals relating to any copper binding role *in vivo*. The interaction of full-length and truncated forms of the prion protein with copper (II) has been investigated by a range of techniques including EPR

[20-22], CD [23], X-ray crystallography[24], NMR [25, 26], mass-spectrometry [14, 15], Raman [27, 28], FT-IR [29] and potentiometry [30]. A consensus has emerged that at maximum copper (II) occupancy the prion protein can bind five or six copper ions, and that each of these ions is coordinated by a single histidine imidazole and two deprotonated backbone amide nitrogen atoms [14, 21, 24]. In this way each of the four octapeptide repeats can bind a single ion, and sites at histidines 96 and 111 can bind an additional two ions in a similar fashion [21, 26]. It has however become clear that at lower copper occupancy, copper coordination by the octapeptide repeats is different to the total occupancy state. Three published works now report that within the four octapeptide repeats, a single copper (II) ion can be coordinated by multiple histidine imidazoles without the involvement of backbone amides [25, 30, 31]. Most estimates of the affinity of PrP for copper have been in the low micromolar range [15, 23, 32, 33], but the affinity has also been placed dramatically higher, in the femtomolar range in idealised conditions [25]. In the absence of definitive *in vivo* experiments which might confirm that PrP is a true cuproprotein, *in vitro* affinity measurements offer an alternative route to assess if this hypothesis is credible. *In vivo,* most extra-cellular copper is sequestered in complexes with proteins and amino acids which have affinities in the nanomolar to picomolar range [34, 35], suggesting that if PrP does have only a micromolar affinity for copper it would be would be unlikely to bind copper under normal physiological conditions.

We have used equilibrium dialysis to thoroughly characterise the multiple modes of copper coordination which can occur in peptides representing residues 57-91 (containing the four octapeptide repeats) and residues 91 -115 (containing histidine residues 96 and 111) of the human prion protein. As well as allowing the determination of stoichiometry, this technique can be used to identify sites of different affinity through Scatchard analysis and provides a framework for the unambiguous interpretation of spectroscopic measurements. In order to keep copper (II) soluble above about pH 5, a chelating buffer must be used. As these buffers also compete against any interaction of copper (II) with the peptide, the experiment reports an apparent affinity that is weakened relative to the true value. In each case the true dissociation constants has been calculated by determining the free copper concentration when the total copper concentration is the same as the apparent dissociation constant. We have used this information, in conjuction with circular

dichroism, fluorescence and NMR spectroscopic measurements to characterize the multiple modes in which copper (II) can be coordinated by the PrP peptides. The data reveal that the affinities of the lower occupancy copper binding modes are in the nanomolar range. This work demonstrates for the first time that multiple modes of copper (II) coordination can occur at the binding sites outside of the octapeptide repeats, and that self association plays a role in the highest affinity copper binding mode of both peptides.

Materials and Methods

Peptide Synthesis and Purification

Peptide synthesis was carried by ABC, Imperial College London. Peptides were produced by solid phase step-wise synthesis using the Fmoc N-terminal protection strategy. All peptide products were purified and analyzed by reverse phase HPLC. Molecular weight determination was performed by MALDI mass spectrometry. Both peptides were acetylated at the N-terminus and amidated at the C-terminus. The peptide sequences used were: PrP^{57-91}- WGQPHGGGWG QPHGGGWGQP HGGGWGQPHG GGWGQ; PrP^{91-115}- QGGGTHSQWN KPSKPKTNMK HMAGA.

Equilibrium Dialysis

Solutions of peptides in either 5 mM Tris pH 7.4, 50 mM MOPS pH 7.4 or 10 mM acetate, pH 5.5 were dialyzed for approximately 10 hours against a one liter reservoir of copper containing buffer, using Spectra/Por 7 3500 MWCO dialysis membrane. Copper was added to each buffer reservoir from a stock of either 20 mM $CuSO_4$ or 20 mM $CuSO_4$ containing 40 mM glycine, to achieve the desired copper concentration. After dialysis, samples of the peptide solution and the dialysis buffer were diluted 5 fold with 1% Aristar nitric acid and the copper concentration then measured using a Spectro-Ciros CCD ICP atomic emission spectrometer. Typically, final peptide concentrations were *ca.* 10 μM for PrP^{57-91} and *ca.* 40 μM for PrP^{91-115}.

Measurements of peptide concentrations

Peptide concentrations were determined by measuring the absorbance of solutions at 280 nm using the molar extinction coefficient of tryptophan at that wavelength. For experiments on PrP^{91-115} at pH 7.4, the contribution of peptide bound copper to the extinction coefficient at 280 nm was significant. The extinction coefficient of copper (II) in the $(Cu)_2PrP^{91-115}$ complex was measured as 1700 M^{-1} cm^{-1} and a similar value was obtained for the $Cu(PrP^{91-115})_2$ complex. The concentration of peptide bound copper was determined directly from the ICP-AES results and thus the contribution of the peptide bound copper to the absorbance at 280 nm could be calculated and subtracted from the raw data.

Circular Dichroism

Spectra were recorded on a Jasco J-810 spectropolarimeter at 25 ºC, with a scanning speed of 10 nm /min and the slit width set to 150 μm. Signal to noise was limited in most samples and so to average out noise as much as possible, the data pitch was set to 5 nm, the integration time to 30 seconds per point and the number of scans per spectrum to four. Aliquots of 2 mM or 20 mM $CuSO_4$ were added to peptide solutions in Tris and NEM buffers. For peptide samples in MOPS buffer, copper was added as a glycine chelate either as 2 mM $CuSO_4$, 4 mM glycine, or 20 mM $CuSO_4$, 40 mM glycine. CD measurements in mdeg (θ) were converted to molar circular dichroism (Δε, with units of liter mol^{-1} cm^{-1}) using the relationship $\Delta\varepsilon = \theta / (33{,}000.l.c)$, where c is the concentration in moles per litre and l is the pathlength in cm.

Fluorescence Spectroscopy

Experiments were carried out on a Cary Eclipse fluorimeter at 25 ºC, with the excitation and emission wavelengths set to 280 nm and 356 nm**,** respectively**.** The excitation slit width was 5 μm for all experiments. The emission slit width was 10 μm for experiments on $PrP^{57\text{-}91}$ and 5 μm for $PrP^{91\text{-}115}$. The detector voltage was set to either 600 or 800 V to bring the initial fluorescence of the sample into a measurable range. Peptide solutions were titrated with either 1 mM $CuSO_4$ in 5 mM Tris, pH 7.4 ($PrP^{57\text{-}91}$) or 10 mM $CuSO_4$ in 50 mM Tris, pH 7.4 (for $PrP^{91\text{-}115}$). Data were corrected for the dilution of the sample.

NMR

$PrP^{57\text{-}91}$ samples contained 30 μM peptide in 25 mM phosphate buffer, pH 7.4 and were titrated with aliquots of 200 μM copper bis-glycinate or 1M MOPS, pH 7.4. To exclude pH changes as a cause of the observed chemical shift changes, the titration with MOPS was repeated in 50 mM phosphate buffer, pH 7.4. The $PrP^{91\text{-}115}$ sample contained 100 μM peptide in 5 mM Tris, pH 7.4 and was titrated with 1mM $CuSO_4$ in the same buffer. Both samples contained 5 % D_2O. Spectra of $PrP^{57\text{-}91}$ were recorded on a Bruker DRX-600 spectrometer whilst spectra of $PrP^{91\text{-}115}$ were recorded on a DRX-500 instrument. Both spectrometers were equipped with cryoprobes. Water suppression was achieved by pre-saturation of the water resonance. The recycle delay was set to allow complete relaxation of the peptide resonances between scans. For $PrP^{57\text{-}91}$ a 4 second recycle delay was used, whilst a 6 second delay was necessary for

PrP^{91-115}. All spectra were recorded at 25 ºC.

Simulations of equilibria for formation of metal complexes and calculations of dissociation constants

Simulations were carried out using an in house program to numerically calculate the equilibrium position of a series of linked equilibria, given fixed total concentrations of metal and ligand. In the simulations of binding to PrP^{57-91} shown in Figure 6 the four independent sites (termed mode C) were modeled using macroscopic dissociation constants of 0.25, 0.66, 1.5 and 4.0 μM, likewise the two independent sites (termed mode B) were modeled using macroscopic dissociation constants of 125 and 500 nM.

To obtain the non-linear fits to the Scatchard plots shown in Figure 7B and 7C the K_d values were first crudely estimated by iteratively adjusting the K_d parameters in the model. The final fit was obtained by running a suite of simulations to sample, to one significant figure, all possible combinations of the two or three K_d parameters. For example, for the data in Figure 7B the parameters were set to: 10, 20, 30, 40 and 50 μM for K_d^1; 3, 4, 5, 6 and 7 μM for K_d^2; and to 20, 30, 40 and 50 μM for K_d^3, giving 100 data sets in total. The best fit to the observed data from these calculated data sets was then selected by least squares fitting. The linear fits to the other Scatchard plots were also calculated by least squares fitting.

The true dissociation constant of each peptide:copper complex is taken to be the concentration of free copper in the buffer solution when the total copper concentration is equal to the observed apparent dissociation constant. The acetate ion forms a 1:1 complex with copper (II) with a dissociation constant of 4.2 mM [36]. Since the acetate concentration is in excess of the copper concentration, the fraction of free copper in the acetate buffer can be calculated using the following relationship, which is derived from the standard binding equation for formation of a 1:1 complex:

$$\frac{M_{free}}{M_{total}} = 1 - \frac{L_{free}}{K_d + L_{free}} \approx 1 - \frac{L_{total}}{K_d + L_{total}} \quad (\text{when } L_{total} >> M_{total})$$

M_{free} = free metal concentration M_{total} = total metal concentration

L_{free}= free ligand concentration L_{total}= total ligand conentration

Glycine and Tris form 2:1 and 4:1 complexes with copper (II) respectively and so a mixture of different complexes is present in each case. The calculation of the free copper concentration in these buffers is more complex and had to be carried out using the same numerical model described above. Equilibria describing the formation of the $Cu(Tris)_4$ complex and the Cu bis-glycinate complex were modeled using stepwise dissociation constants from the literature [36] adjusted for pH [37]. For Tris these constants are 0.55, 1.0, 1.7 and 4.9 mM and for glycine they are 1.2 and 12 μM.

Results

At maximum occupancy PrP^{57-91} binds four copper (II) metal ions

Titration of PrP^{57-91} with copper (II) in NEM buffer at pH 7.4 produces a complex with strong CD bands at 350 and 580 nm (Figure 1A). The CD signal saturates at a stoichiometry of 4:1. When the signal intensity is plotted against the quantity of copper added it can be seen that the increase does not relate linearly to the quantity of copper (Figure 1B); the change in the CD signal on adding one mole equivalent of copper (II) is substantially smaller than for subsequent additions. These findings are in agreement with previous studies [20, 23].

The choice of buffer is important in these experiments. Whereas NEM and other morpholine based buffers interact only very weakly with copper (II) [37], buffers that compete more strongly for copper (II), such as Tris, will prevent formation of the CD active complex at equivalent copper concentrations [23]. Accordingly, we have found that addition of 0.5 mM glycine in NEM buffer to the 4:1 complex at pH 7.4 abolishes about 80 % of the CD signal (data not shown). The fact that the four copper sites in the octapeptide repeats in PrP^{57-91} are not maintained in the presence of glycine, is consistent with the low reported affinities which are in the micromolar range [15, 23]. However, the absence of a substantial CD signal after the addition of one mole equivalent copper (II) to the peptide in NEM buffer, does not preclude the existence of a single site of higher affinity.

PrP^{57-91} coordinates a single copper (II) with higher affinity

Equilibrium dialysis shows that a single copper (II) ion will bind to PrP^{57-91} in Tris buffer at pH 7.4 (Figure 2A) with higher affinity than observed at additional sites. The apparent dissociation constant in 5 mM Tris is 1.0 ± 0.2 μM, and using the association constants for the formation of a $Cu(Tris)_4$ complex [36], it can be calculated that 1 μM total copper (II) will give ~3 nM free copper (II) in this buffer. Thus, the dissociation constant for the $Cu(PrP^{57-91})$ complex can be estimated as 3 ± 2 nM (apparent and true dissociation constants for PrP^{57-91} are summarised in table 2). Using the equilibrium dialysis data, peptide samples can be prepared for spectroscopic analysis under conditions where the amount of bound copper is accurately known. In this case the 1:1 complex was found to produce virtually no CD signal at visible

wavelengths (Figure 2C), and the form of coordination present can therefore not resemble that observed at maximum occupancy. The data also shows further binding can occur in these conditions (Figure 2A) but with a substantially lower affinity.

A single copper (II) binding site is also detected in acetate buffer at pH 5.5 (Figure 2B). In 10 mM acetate the apparent dissociation constant is 13 ± 2 μM, and from this the dissociation constant of the Cu(PrP^{57-91}) at pH 5.5 can be calculated as 4 ± 2 μM. This 1:1 complex also has no detectable CD signal at 580 nm (Figure 2C), suggesting an indistinguishable mode of metal coordination to that observed at pH 7.4.

The PrP^{57-91} peptide forms a 1:1 complex with copper (II) in which all four histidines are coordinated

To investigate the nature of the 1:1 complex, a sample of PrP^{57-91} was titrated with copper (II) and observed by 1D proton NMR. Copper (II) is paramagnetic and will cause NMR signals from nearby nuclei to broaden to the point of becoming undetectable. The addition of copper caused specific, simultaneous broadening of all histidine imidazole resonances in PrP^{57-91} (Figure 3). This indicates that all four histidine sidechains in the peptide are involved in coordinating the first copper (II) ion. Coordination by four imidazoles is consistent with the observed 1:1 stoichiometry of the highest affinity binding event. The CD response arises from copper (II) coordination in a chiral environment, which in this case occurs predominantly due to the chiral C_α centre between the coordinating imidazole and backbone amide of the histidine. In a multiple imidazole coordinated species, the metal ion would be substantially further from this chiral centre compared to coordination through both the imidazole and the backbone amide. Thus, the weak CD signal observed for the 1:1 complex is also consistent with multiple histidine coordination. Finally, imidazole only coordination would be substantially less pH sensitive than backbone amide coordination due to the lower pK_a of the imidazole group. If the pH is below the pK_a of a coordinating group in a metal binding site, the affinity of the site is reduced by a factor of ten for each pH unit below the pK_a. Since the pK_a of the imidazole group is approx. 6, and the site is believed to contain four imidazole groups, the affinity of the complex would be expected to be reduced by a factor of about a hundred (i.e. $10^{4*(6.0-5.5)}$) at pH 5.5 relative to pH 7.4. The observed

difference is in fact ~1000 fold, suggesting that other factors may also be involved.

Low copper occupancy causes self association of PrP^{57-91}

Although the 1:1 complex does not produce CD bands at visible wavelengths, it is readily observed by a reduction in the intrinsic tryptophan fluorescence of the peptide (Figure 4). We also found that the relative reduction in the fluorescence of PrP^{57-91}, that occurs upon titration with copper, is dependent on the peptide concentration. The greater degree of fluorescence quenching that occurs at higher peptide concentrations is consistent with a greater fraction of peptide being held in close proximity to a copper (II) ion. The peptide concentration affects both the rate at which fluorescence is quenched by addition of copper, and the fluorescence at the endpoint of the titration, where all the peptide should be in the 1:1 complex, $Cu(PrP^{57-91})$. A simple explanation for this is that $Cu(PrP^{57-91})$ can associate with other molecules of apo-peptide, at low copper concentrations, or with other $Cu(PrP^{57-91})$ complexes. Since the changes in the fluorescence quenching behavior are seen on increasing the peptide concentration from 30 nM to 1 μM, the apparent dissociation constant for the self association process will be within this range. It is likely that copper (II) will dissociate from these self-associated peptide complexes more slowly than from the monomeric complex. If this is the case the self-association process will enhance the apparent affinity of copper (II) binding in the 1:1 complex. Indeed at 30 nM peptide concentration the titration data shows half maximal binding at a copper concentration of approximately 4 μM, whilst at a peptide concentration of 1 mM it is 1.5 μM.

PrP^{57-91} can coordinate two copper (II) ions with intermediate affinity

Equilibrium dialysis carried out in MOPS buffer at pH 7.4 where the copper was presented as a glycine chelate revealed a clear 2:1 stoichiometry (Figure 5A). In this case the two sites have identical apparent dissociation constants of 6 ± 2 μM and, given stepwise dissociation constants for copper bis(glycinate) of 1.2 μM and 12 μM [37], a true dissociation constant of 250 ± 50 nM. In contrast to the 1:1 complex formed in Tris buffer, the CD spectrum of the 1:1 complex formed in this buffer has clear bands in the visible region at 350 and 580 nm (Figure 5C), indicating a different mode of copper (II) coordination.

We judged that the most probable cause of the alternate copper coordination in this

1:1 complex was an interaction between the peptide and the MOPS buffer which interferes with copper coordination; we had previously observed that the peptide is insoluble in the presence of MES (chemically similar to MOPS) at pH 5.5 whilst it is soluble in other buffers at the same pH. To test the proposal that the peptide interacts with MOPS, a sample of the peptide was titrated with MOPS buffer at pH 7.4 and observed by NMR. Chemical shift changes were indeed observed for the aromatic histidine signals (Figure 5B) confirming that an interaction does occur and that the bound species is significantly occupied at a MOPS concentration of 50 mM, equivalent to that present in the equilibrium dialysis and CD experiments described above.

The CD spectrum of the 2:1 complex formed in MOPS buffer has peaks at the same wavelengths as the 1:1 complex but with twice the intensity, again implying that the two sites are identical. Interestingly, the positions of these CD bands are very similar to those seen previously for the $Cu_4(PrP^{57-91})$ complex in NEM buffer at pH 7.4. The relative signal intensity of the $Cu_2(PrP^{57-91})$ complex in MOPS is also comparable to that seen for the $Cu_4(PrP^{57-91})$ complex, suggesting a similar mode of metal coordination. However, the metal coordination cannot be identical since binding of PrP^{57-91} in MOPS saturates at a stoichiometry of 2:1 rather than 4:1 and the two sites are of sufficiently high affinity to form in the presence of glycine.

Simulations of copper binding to PrP^{57-91} with three modes of coordination

To test the counter-intuitive conclusion that when the two forms of binding are mutually exclusive four weak copper (II) binding sites can out compete a single higher affinity site, we have used our experimentally derived dissociation constants to simulate the populations of the different species over a range of total copper (II) concentrations (Figure 6). The following equilibrium was modeled, where three mutually exclusive modes of binding are possible, which here are labeled A, B and C:

$$\begin{array}{ccccccccccc} Cu^{A}P & \leftrightarrow & P & \leftrightarrow & Cu^{C}P & \leftrightarrow & Cu^{C}{}_2P & \leftrightarrow & Cu^{C}{}_3P & \leftrightarrow & Cu^{C}{}_4P \\ & & \updownarrow & & & & & & & & \\ & & Cu^{B}P & & & & & & & & \\ & & \updownarrow & & & & & & & & \\ & & Cu^{B}{}_2P & & & & & & & & \end{array}$$

A dissociation constant of 3 nM was used for the single site present in mode A and a microscopic dissociation constant of 250 nM for the two indpendent sites available in mode B, both based on our experimental measurements. A microscopic dissociation constant of 1 μM was used for each of the four independent sites available in mode C, based on literature reports of the affinity of this mode of binding [32]. The total peptide concentration was set to 30 μM to be equivalent to the CD experiments shown in Figure 1. With one mole equivalent of Cu^{2+}, 94% of the peptide was in the high affinity $Cu^{A}P$ complex, which represents the multiple histidine coordinated complex we have described. When the total copper concentration is increased the higher stoichiometry, lower affinity binding becomes dominant; with five mole equivalents of Cu^{2+} present 97 % of the peptide is in either the $Cu^{C}{}_{3}P$ or $Cu^{C}{}_{4}P$ forms, which represent complexes where each copper ion is coordinated by de-protonated backbone amides and a single histidine imidazole. The model therefore supports the assertion that four binding sites of micromolar affinity can out compete a single site of nanomolar affinity. Furthermore, if the presence of the mode A species was not taken into account, the populations of the mode C species would appear to show cooperative binding. The population of the two intermediate affinity sites (mode B- $Cu^{B}P$, $Cu^{B}{}_{2}P$), with 250 nM affinity, does not exceed 15 % of the total peptide concentration at any point. It is possible that the intermediate affinity form of binding (mode B) is stronger than we have estimated. If the interaction of the peptide with the MOPS buffer competes against this mode of binding, then the dissociation constant will be lower than 250 nM in the absence of MOPS.

At maximum occupancy $PrP^{91\text{-}115}$ can bind two copper (II) ions

A similar program of experiments to that described for $PrP^{57\text{-}91}$ was carried out on the peptide $PrP^{91\text{-}115}$ to determine if this peptide could also access multiple copper (II) binding modes. Equilibrium dialysis data for $PrP^{91\text{-}115}$ in MOPS buffer at pH 7.4 with copper presented as a glycine chelate, indicates that two sites of equivalent affinity are present (Figure 7A) with apparent dissociation constants of 6 ± 1 μM and true dissociation constants 250 ± 30 nM. The CD spectrum of the $(Cu)_2$ $PrP^{91\text{-}115}$ complex which forms in MOPS buffer (Figure 7D) is very similar to that reported by Jones *et al.* with a large positive band at around 500 nm. It has been demonstrated by others that this complex comprises two copper binding sites, each involving coordination by a single histidine imidazole, from either histidine 96 or 111, and nearby backbone

amide groups [21, 26].

PrP^{91-115} will form a $Cu(PrP^{91-115})_2$ complex

We investigated the binding interaction of PrP^{91-115} with copper in Tris buffer at pH 7.4 by equilibrium dialysis and extrapolation from the first three points of the Scatchard plot shows that the highest affinity interaction has a stoichiometry of 0.5:1 (Figure 7B). This indicates that at low copper concentrations each copper ion forms a complex with two peptide molecules. The equations describing the Scatchard plot for formation of such a species are non linear. In order to estimate values for the dissociation constants describing the formation of the $Cu(PrP^{91-115})_2$ species, the following equilibrium was modeled:

$$\begin{array}{ccccc} & & K_{d1} & & K_{d2} & \\ P & \leftrightarrow & CuP & \leftrightarrow & CuP_2 \\ & & \updownarrow K_{d3} & & \\ & & Cu_2P & & \end{array}$$

Using this model, values for the dissociation constants could be fitted to the Scatchard plot, and thus K_{d1} was estimated as 30 ± 10 μM, K_{d2} as 5 ± 1 μM and K_{d3} as 40 ± 10 μM. As the K_{d1} and K_{d3} values describe the binding of free copper to the peptide these values are apparent dissociation constants. The true values were then calculated as 100 ± 50 nM and 140 ± 50 nM respectively (apparent and true dissociation constants for PrP^{91-115} are summarised in table 2). The fact that different complexes are again observed in Tris and MOPS buffers points to an interaction between the MOPS buffer and the peptide that competes against formation of the $Cu(PrP^{91-115})_2$ complex.

The complexes of PrP^{91-115} with copper are detectable by fluorescence (Data Not Shown). The effects of titration of this peptide with copper are again dependent on the peptide concentration, supporting the other evidence for the existence of $Cu(PrP^{91-115})_2$ complex.

The mode of copper coordination in the $Cu(PrP^{91-115})_2$ complex is pH dependent

A $Cu(PrP^{91-115})_2$ complex will also form at pH 5.5 in 10 mM acetate buffer (Figure 7C). At this pH there was no evidence of a $Cu_2(PrP^{91-115})$ complex and therefore a

simplified version of the above equilibrium, which did not contain the Cu_2P species, was fitted to the data to give dissociation constants of 1 ± 0.1 mM for K_{d1} and of 40 ± 10 μM for K_{d2}. The true value for K_{d1} was then calculated as 300 ± 100 μM, some 4000 fold weaker at pH 5.5 than at pH 7.4. The amide functional group has a pK_a well above 7.4, and so if two deprotonated amides and a single imidazole are involved in coordinating the metal ion, then the affinity at pH 5.5 would be a factor of around 2×10^4 lower than at pH 7.4 (i.e. $10^{(2 \times (7.4 - 5.5)) + (6.0 - 5.5)}$). The fact that the reduction in affinity is not this great could indicate that at pH 5.5 the dominant $Cu(PrP^{91-115})$ species is a complex with coordination from two histidine imidazole groups. The binding of a second peptide to the $Cu(PrP^{91-115})$ complex to give $Cu(PrP^{91-115})_2$ is about tenfold weaker at pH 5.5 than at pH 7.4, this would be consistent with coordination of the copper (II) ion by two imidazoles from the second peptide, since pH 5.5 is 0.5 units below the histidine imidazole pK_a. Interestingly, at pH 5.5 the second peptide binds with higher affinity than the first, an observation which could be rationalized if a direct interaction between the peptides stabilised the Cu_2P species.

The $Cu(PrP^{91-115})_2$ complexes at pH 7.4 and pH 5.5 both produce a CD signal at visible wavelengths (Figure 7D) but the spectra are not identical, indicating that copper (II) coordination is affected by pH. If these spectra were normalized by the concentration of bound copper instead of the concentration of peptide, the band at 525 nm would be similar to the bands seen in the $Cu_2(PrP^{91-115})$ complex. This would be consistent with some backbone amide coordination occurring in the $Cu(PrP^{91-115})_2$ complexes.

Investigation of the $Cu(PrP^{91-115})_2$ complex by NMR

In an effort to confirm which functional groups were involved in coordinating copper in the $Cu(PrP^{91-115})_2$ complex, a titration of the peptide with copper (II) was observed by NMR, similar to that already described for PrP^{57-91}. In this titration, signals originating from both histidine imidazole sidechains were observed to broaden simultaneously as copper was added to the sample (Figure 8A) indicating that they are both involved in the $Cu(PrP^{91-115})_2$ complex. The relative populations of free peptide and the different metal complexes can be predicted based on the dissociation constants fitted to the equilibrium dialysis data (Figure 8B). The total integral of the Hδ2 signal does not decrease on addition with copper to the same extent as the

population of free peptide. This must be because not all the histidine signals in the $Cu(PrP^{91-115})_2$ complex are broadened beyond detection. This would be the case if of the four histidine residues in the two peptides, one or two did not directly coordinate copper. At least two histidine signals must become undetectable in the $Cu(PrP^{91-115})_2$ complex, if only one was affected, the reduction in signal in the first part of the titration would be about half that observed. In summary, in the $Cu(PrP^{91-115})_2$ complex the copper (II) ion must be coordinated by either two or three histidine side chains, and probably also with a contribution from de-protonated backbone amides.

Discussion

The four octapeptide repeats in the peptide PrP^{57-91} can bind copper in at least three different ways (Figure 9A). This has recently been reported by other investigators who have used EPR data to show that three species exist and to propose the mode of coordination in each [31]. Our data support their proposals and allow us to build on the work in several important ways. Firstly we have been able to directly estimate the affinity of the two higher affinity modes of copper (II) binding. We have shown that self association of the octapeptide repeats plays a role in the highest affinity, multiple histidine coordination mode. We have also defined conditions under which the two intermediate affinity sites are the only species present, which was reported to be an obstacle to further spectroscopic investigation of this species by Chattopadhyay *et al*. The CD spectra that we were able to acquire for the $Cu_2(PrP^{57-91})$ complex support the proposal that the copper is coordinated in this complex in a similar way as the $Cu_4(PrP^{57-91})$ complex , but with an additional axially coordinated histidine.

From our data it is also clear that at least two forms of copper coordination occur in the peptide PrP^{91-115} (Figure 9B). At maximum occupancy two sites are observed which both involve coordination by a histidine imidazole and deprotonated backbone amides. The affinities of these two sites are similar, indeed they could be the same within error, and are in the range of 100 to 200 nM. The $Cu(PrP^{91-115})$ complex binds a second peptide with an affinity of around 5 μM; an affinity this high suggests that the second peptide is acting as a bidentate ligand because a single imidazole only binds to copper with a dissociation constant of about 60 μM [37]. The pH dependence of this interaction also supports the idea that two imidazoles from the second peptide coordinate the copper (II) ion. The interaction could take the form of axial coordination from two imidazole groups or could involve the displacement of some of the backbone amides that coordinate copper in the $Cu(PrP^{91-115})$ complex.

The existence of the $Cu(PrP^{91-115})_2$ complex strongly suggests that the copper ion in the $Cu(PrP^{91-115})$ complex has spare coordination sites that can bind a second peptide molecule through its histidine residues. As such the peptide PrP^{91-115} can not be considered a complete model of copper (II) binding in the full-length protein, where additional histidine sidechains would be available to fill any spare coordination sites.

Likewise the self-associative behaviour of the Cu(PrP^{57-91}) complex could be explained if there were spare coordination sites on the metal ion that allowed intermolecular complexes to form. Again in the full length protein, with additional histidine sidechains available, extra coordinating groups may be involved in the complex. If this were the case, affinities in the full-length protein would be higher than those measured in the peptide models used in this study.

Our observations of multiple copper (II) coordination modes in the octapeptide repeats explain discrepancies in the literature about the stoichiometry of copper (II) binding in the octapeptide repeats and in the full length protein. As described earlier, most studies have reported that the four octapeptide repeats bind four copper (II) ions with micromolar affinities at pH 7.4 [15, 20, 23]. Likewise a stoichiometry of 5.2 ± 1.1 has been observed for the full length prion protein at pH 7.4 [21]. These high occupancy binding modes, which have affinities in the micromolar range, will only occur in the absence of competition for copper (II) from chelating agents, such as Tris or glycine. Studies that use conditions that compete against the high occupancy copper (II) binding modes, such as amino acid competition or gel-filtration chromatography, have reported that the four octapeptide repeats can bind only a single copper (II) ion [12, 25]. Similarly, mildly acidic pH will disfavor the deprotonation of backbone amides which is required for high-occupancy binding; at pH 6.0 the full length protein is found to bind just two copper ions [33] instead of the five or six at pH 7.4. It is now clear that these low occupancy copper (II) binding modes involve coordination from multiple histidine imidazoles, which allows the sites to be maintained at lower pH, and that they have affinities in the low nanomolar range, which is sufficiently strong for the site to remain intact in the presence of competition from chelating agents with micromolar affinities.

The total copper concentration in serum is 16-20μM, all of which exists as complexes - the majority with caeruloplasmin and the remainder with other proteins (including transcuprein and albumin), peptides and amino acids [34] – and the concentration of free copper (i.e. an aqua complex) is therefore virtually nil. On the cell surface in brain tissue, PrP would equilibrate with the extra-cellular pool of copper available in the brain interstitial fluid, which is in equilibrium with the CSF. In healthy subjects

the copper concentration in the CSF is of the order of 0.1 μM [38], and again this is expected to exist as complexes with albumin, caeruloplasmin or amino acids. Therefore, in determining if PrP is an authentic cuproprotein, its affinity should be compared to the affinities of the other copper binding species in the extra-cellular milieu, with which it must compete for copper, and not the total copper concentration. The dissociation constant of human albumin for copper (II) is about 10 pM [35], whilst the step wise dissociation constants for the formation of a copper bis-histidinate complex at pH 7.4 are about 4 nM and 0.5 μM [37]. Histidine is present at around 10 μM concentration in the CSF, and albumin is present at about 20 mg/dl which equates to about 3 μM. Thus, both these species are well in excess of the total copper (II) concentration and have similar or higher affinities than the peptide models of the prion protein we have studied. Our measured affinities therefore suggest that only a small fraction of PrP, if any, is likely to bind copper under normal conditions in the central nervous system. However, during neuronal depolarization, copper concentration at the synapse increases; one estimate places this increase as *ca.* 15 μM, with about 20 % of this is in complexes with dissociation constants weaker than 100 nM [39]. It is thus likely that PrP could bind copper only when levels are elevated during neuronal depolarization. Even in this circumstance though, probably only the higher affinity binding modes would be populated due to the excess of other species which can bind copper (II) with micromolar or higher affinities.

Our study also raises the possibility that the elevated copper levels which occur during neuronal depolarization could play a role in controlling self-association of PrP *in vivo*, if the effective molarity of PrP on the cell surface is higher than about 100 nM. Any factor that could influence the self-association of PrP *in vivo* is of potential importance in understanding the normal function of PrP^C and its role in prion disease and thus would merit further investigation.

Acknowledgements

This work was funded by the UK Medical Research Council and Biotechnology and Biological Sciences Research Council. We would like to thank Ray Young for the preparations of figures, Neil Brammal for assistance with ICP-emission spectrometry, Andrea Hounslow for assistance with NMR spectroscopy and Matthew Cliff and Rosie Staniforth for critical reading of the manuscript.

Abbreviations

ICP-AES, Inductively Coupled Plasma - Atomic Emission Spectrometry; K_d , dissociation constant; NEM, N-ethyl morpholine; PrP, prion protein; PrP^C, cellular isoform; PrP^{57-91}, PrP^{91-115} , peptides representing residues 57-91 and residues 91-115 of the human prion protein respectively; Copper complexes are shown using a variation of standard chemical nomenclature, e.g. $Cu(PrP^{57-91})_2$, a complex of PrP^{57-91} with two copper ions; $Cu(PrP^{91-115})_2$, a complex of a copper ion with two PrP^{91-115} molecules.

References

1 Collinge, J. (2001) Prion diseases of humans and animals: Their causes and molecular basis. Annu. Rev. Neurosci. **24**, 519-550

2 Griffith, J. S. (1967) Self-replication and scrapie. Nature (London) **215**, 1043-1044

3 Prusiner, S. B. (1982) Novel Proteinaceous Infectious Particles Cause Scrapie. Science **216**, 136-144

4 Stahl, N., Borchelt, D. R., Hsiao, K. and Prusiner, S. B. (1987) Scrapie Prion Protein Contains a Phosphatidylinositol Glycolipid. Cell **51**, 229-240

5 Riek, R., Hornemann, S., Wider, G., Billeter, M., Glockshuber, R. and Wuthrich, K. (1996) NMR structure of the mouse prion protein domain PrP(121-321). Nature (London) **382**, 180-182

6 Zahn, R., Liu, A. Z., Luhrs, T., Riek, R., von Schroetter, C., Garcia, F. L., Billeter, M., Calzolai, L., Wider, G. and Wuthrich, K. (2000) NMR solution structure of the human prion protein. Proc. Natl. Acad. Sci. U. S. A. **97**, 145-150

7 Bendheim, P. E., Brown, H. R., Rudelli, R. D., Scala, L. J., Goller, N. L., Wen, G. Y., Kascsak, R. J., Cashman, N. R. and Bolton, D. C. (1992) Nearly ubiquitous tissue distribution of the scrapie agent precursor protein. Neurology. **42**, 149-156

8 Dodelet, V. C. and Cashman, N. R. (1998) Prion protein expression in human leukocyte differentiation. Blood. **91**, 1556-1561

9 Bueler, H., Fischer, M., Lang, Y., Bluethmann, H., Lipp, H. P., Dearmond, S. J., Prusiner, S. B., Aguet, M. and Weissmann, C. (1992) Normal Development and Behavior of Mice Lacking the Neuronal Cell-Surface Prp Protein. Nature (London) **356**, 577-582

10 Collinge, J., Whittington, M. A., Sidle, K. C. L., Smith, C. J., Palmer, M. S., Clarke, A. R. and Jefferys, J. G. R. (1994) Prion Protein Is Necessary for Normal Synaptic Function. Nature (London) **370**, 295-297

11 Tobler, I., Gaus, S. E., Deboer, T., Achermann, P., Fischer, M., Rulicke, T., Moser, M., Oesch, B., McBride, P. A. and Manson, J. C. (1996) Altered circadian activity rhythms and sleep in mice devoid of prion protein. Nature

(London). **380**, 639-642

12 Hornshaw, M. P., McDermott, J. R. and Candy, J. M. (1995) Copper-Binding to the N-Terminal Tandem Repeat Regions of Mammalian and Avian Prion Protein. Biochem. Biophys. Res. Commun. **207**, 621-629

13 Hornshaw, M. P., McDermott, J. R., Candy, J. M. and Lakey, J. H. (1995) Copper-Binding to the N-Terminal Tandem Repeat Region of Mammalian and Avian Prion Protein - Structural Studies Using Synthetic Peptides. Biochem. Biophys. Res. Commun. **214**, 993-999

14 Qin, K. F., Yang, Y., Mastrangelo, P. and Westaway, D. (2002) Mapping Cu(II) binding sites in prion proteins by diethyl pyrocarbonate modification and matrix-assisted laser desorption ionization-time of flight (MALDI-TOF) mass spectrometric footprinting. J. Biol. Chem. **277**, 1981-1990

15 Whittal, R. M., Ball, H. L., Cohen, F. E., Burlingame, A. L., Prusiner, S. B. and Baldwin, M. A. (2000) Copper binding to octarepeat peptides of the prion protein monitored by mass spectrometry. Protein Sci. **9**, 332-343

16 Brown, D. R., Qin, K. F., Herms, J. W., Madlung, A., Manson, J., Strome, R., Fraser, P. E., Kruck, T., vonBohlen, A., SchulzSchaeffer, W., Giese, A., Westaway, D. and Kretzschmar, H. (1997) The cellular prion protein binds copper in vivo. Nature (London) **390**, 684-687

17 Waggoner, D. J., Drisaldi, B., Bartnikas, T. B., Casareno, R. L. B., Prohaska, J. R., Gitlin, J. D. and Harris, D. A. (2000) Brain copper content and cuproenzyme activity do not vary with prion protein expression level. J. Biol. Chem. **275**, 7455-7458

18 Rachidi, W., Vilette, D., Guiraud, P., Arlotto, M., Riondel, J., Laude, H., Lehmann, S. and Favier, A. (2003) Expression of prion protein increases cellular copper binding and antioxidant enzyme activities but not copper delivery. J. Biol. Chem. **278**, 9064-9072

19 Pauly, P. C. and Harris, D. A. (1998) Copper stimulates endocytosis of the prion protein. J. Biol. Chem. **273**, 33107-33110

20 Aronoff-Spencer, E., Burns, C. S., Avdievich, N. I., Gerfen, G. J., Peisach, J., Antholine, W. E., Ball, H. L., Cohen, F. E., Prusiner, S. B. and Millhauser, G. L. (2000) Identification of the Cu2+ binding sites in the N-terminal domain of the prion protein by EPR and CD spectroscopy. Biochemistry **39**, 13760-13771

21 Burns, C. S., Aronoff-Spencer, E., Legname, G., Prusiner, S. B., Antholine, W. E., Gerfen, G. J., Peisach, J. and Millhauser, G. L. (2003) Copper coordination in the full-length, recombinant prion protein. Biochemistry **42**, 6794-6803

22 Bonomo, R. P., Imperllizzeri, G., Pappalardo, G., Rizzarelli, E. and Tabbi, G. (2000) Copper(II) binding modes in the prion octapeptide PHGGGWGQ: a spectroscopic and voltammetric study. Chemistry **6**, 4195-4202

23 Viles, J. H., Cohen, F. E., Prusiner, S. B., Goodin, D. B., Wright, P. E. and Dyson, H. J. (1999) Copper binding to the prion protein: Structural implications of four identical cooperative binding sites. Proc. Natl. Acad. Sci. U. S. A. **96**, 2042-2047

24 Burns, C. S., Aronoff-Spencer, E., Dunham, C. M., Lario, P., Avdievich, N. I., Antholine, W. E., Olmstead, M. M., Vrielink, A., Gerfen, G. J., Peisach, J., Scott, W. G. and Millhauser, G. L. (2002) Molecular features of the copper binding sites in the octarepeat domain of the prion protein. Biochemistry **41**, 3991-4001

25 Jackson, G. S., Murray, I., Hosszu, L. L. P., Gibbs, N., Waltho, J. P., Clarke, A. R. and Collinge, J. (2001) Location and properties of metal-binding sites on the human prion protein. Proc. Natl. Acad. Sci. U. S. A. **98**, 8531-8535

26 Jones, C. E., Klewpatinond, M., Abdelraheim, S. R., Brown, D. R. and Viles, J. H. (2005) Probing copper2+ binding to the prion protein using diamagnetic nickel2+ and 1H NMR: the unstructured N terminus facilitates the coordination of six copper2+ ions at physiological concentrations. J. Mol. Biol. **346**, 1393-1407

27 Miura, T., Hori-i, A., Mototani, H. and Takeuchi, H. (1999) Raman spectroscopic study on the copper(II) binding mode of prion octapeptide and its pH dependence. Biochemistry **38**, 11560-11569

28 Miura, T., Sasaki, S., Toyama, A. and Takeuchi, H. (2005) Copper reduction by the octapeptide repeat region of prion protein: pH dependence and implications in cellular copper uptake. Biochemistry **44**, 8712-8720

29 Gustiananda, M., Haris, P. I., Milburn, P. J. and Gready, J. E. (2002) Copper-induced conformational change in a marsupial prion protein repeat peptide probed using FTIR spectroscopy. FEBS Lett. **512**, 38-42

30 Valensin, D., Luczkowski, M., Mancini, F. M., Legowska, A., Gaggelli, E.,

Valensin, G., Rolka, K. and Kozlowski, H. (2004) The dimeric and tetrameric octarepeat fragments of prion protein behave differently to its monomeric unit. Dalton Trans. 1284-1293

31 Chattopadhyay, M., Walter, E. D., Newell, D. J., Jackson, P. J., Aronoff-Spencer, E., Peisach, J., Gerfen, G. J., Bennett, B., Antholine, W. E. and Millhauser, G. L. (2005) The octarepeat domain of the prion protein binds Cu(II) with three distinct coordination modes at pH 7.4. J. Am. Chem. Soc. **127**, 12647-12656

32 Kramer, M. L., Kratzin, H. D., Schmidt, B., Romer, A., Windl, O., Liemann, S., Hornemann, S. and Kretzschmar, H. (2001) Prion protein binds copper within the physiological concentration range. J. Biol. Chem. **276**, 16711-16719

33 Stockel, J., Safar, J., Wallace, A. C., Cohen, F. E. and Prusiner, S. B. (1998) Prion protein selectively binds copper(II) ions. Biochemistry **37**, 7185-7193

34 Linder, M. C. (1991) Extracellular Copper Substituents and Mammalian Copper Transport. In Biochemistry of Copper, pp. 73-134, Plenum Press, New York

35 Masuoka, J., Hegenauer, J., Vandyke, B. R. and Saltman, P. (1993) Intrinsic Stoichiometric Equilibrium-Constants for the Binding of Zinc(Ii) and Copper(Ii) to the High-Affinity Site of Serum- Albumin. J. Biol. Chem. **268**, 21533-21537

36 Perrin, D. D. (1979) Stability constants of metal-ion complexes, part B: organic ligands. Pergamon Press, Oxford. Pergamon Press, Oxford

37 Dawson, R. M. C., Elliott, D. C., Elliott, W. H. and Jones, K. M. (1986) Stability Constants for Metal Complexes. In Data for Biochemical Research, pp. 399-416, Oxford University Press, Oxford

38 Joergstuerenburg, H., Oechsner, M., Schroeder, S. and Kunze, K. (1999) Determinants of the copper concentration in cerebrospinal fluid. J. Neurol. Neurosurg. Psychiatry. **67**, 252-253

39 Hopt, A., Korte, S., Fink, H., Panne, U., Niessner, R., Jahn, R., Kretzchmar, H. and Herms, J. (2003) Methods for studying synaptosomal copper release. J. Neurosci. Methods **128**, 159-172

Tables

pH	buffer	number of sites	K_d app.	K_d real
7.4	5 mM Tris	1	1.0 ± 0.2 μM	3 ± 2 nM
5.5	10 mM acetate	1	13 ± 2 μM	4 ± 2 μM
7.4	50 mM MOPS	2	6 ± 2 μM	250 ± 50 nM

Table 1

Apparent and real dissociation constants for PrP^{57-91}

pH	Buffer	K_d^1 app.	K_d^1 real	K_d^2 real	K_d^3 app.	K_d^3 real
7.4	5 mM Tris	30 ± 10 μM	100 ± 50 nM	5 ± 1 μM	40 ± 10 μM	140 ± 50 nM
5.5	10 mM acetate	1 ± 0.1 mM	300 ± 100 μM	40 ± 10 μM	-	-
7.4	50 mM MOPS	6 ± 1 μM	250 ± 30 nM	-	6 ± 1 μM	250 ± 30 nM

Table 2

Apparent and real dissociation constants for PrP^{91-115}

Figure Legends

Figure 1 A $Cu_4(PrP^{57-91})$ complex is observed by CD

Titration of 30 μM PrP^{57-91} with $CuSO_4$ in 25mM NEM pH 7.4, observed by circular dichroism, reveals a mode of copper binding which produces a strong CD signals at 340 and 580 nm (A). Spectra are shown with 1 to 5 mole equivalents of copper (II) added. The molar circular dichroism at 580 nm is plotted against the mole fraction of copper added showing that copper binding saturates at a stoichiometry of 4:1 (B).

Figure 2 A 1:1 $Cu(PrP^{57-91})$ complex is revealed by equilibrium dialysis with a mode of binding distinct that in the $Cu_4(PrP^{57-91})$ complex

Equilibrium dialysis of PrP^{57-91} shows that the peptide binds a single copper (II) ion with greater affinity than subsequent ones. Scatchard plots show the fractional occupancy (v) against $v/[Cu_{free}]$, with the slope of the fitted lines giving the apparent association constant and the intercept on the x axis giving the number of sites of this affinity. Dialysis against $CuSO_4$ in 5mM Tris, pH 7.4 (A), reveals a single high affinity site (intercept = 0.86) with an apparent dissociation constant of 1.0 ± 0.2 μM. Binding at a second site is observed under these conditions, but is substantially weaker. A single high affinity site (intercept = 1.03) is also present at pH 5.5 in 10 mM acetate buffer (B), with an apparent dissociation constant of 13 ± 2 μM. CD spectra show that these 1:1 complexes involve a different form of coordination to that seen in the 4:1 complex (C). The spectra of the 1:1 complexes formed in 5 mM Tris at pH 7.4 (15 μM PrP^{57-91}, 25 μM $CuSO_4$ –i.e. 1 eq $CuSO_4$ and 10 μM free $CuSO_4$) and in 10 mM acetate of PrP^{57-91} pH 5.5 (42 μM PrP^{57-91}, 300 μM $CuSO_4$ –i.e. 1 eq $CuSO_4$ and 240 μM free $CuSO_4$) – do not give any measurable CD bands, in contrast to the 4:1 complex formed in NEM buffer at pH 7.4.

Figure 3 1D NMR of the $Cu(PrP^{57-91})$ complex

The $Cu(PrP^{57-91})$ complex can be observed by 1D ^1H NMR. The given region of the spectra shows the aromatic histidine and tryptophan signals for a titration of 30 μM peptide with copper bis-glycinate, in 25 mM phosphate pH 7.4. The mole fraction of copper added is shown on the left. Signals from the four histidine residues in the octapeptide repeats are overlapped so only combined signals are observable. Addition

of copper causes specific broadening of the two histidine imidazole signals, with reduced broadening observed for the tryptophan indole signals.

Figure 4 Self-association of the Cu(PrP^{57-91}) complex is demonstrated by fluorescence quenching

The quenching of the intrinsic fluorescence, which occurs on formation of 1:1 complexes of copper and PrP^{57-91} in 5 mM Tris pH 7.4, is dependent on peptide concentration. Samples of PrP^{57-91} were titrated with copper, with peptide concentrations of 3 μM (open circles), 1 μM (filled circles), 0.3 μM (open squares), 0.1 μM (filled squares) and 0.03 μM (open triangles).

Figure 5 A Cu_2(PrP^{57-91}) complex with a mode of binding distinct from both the 1:1 and 4:1 complexes

In MOPS buffer, with copper presented as a glycine chelate, the high affinity 1:1 complex of PrP^{57-91} is disfavored and two identical sites are observed. The Scatchard plot of an equilibrium dialyis experiment in 50 mM MOPS buffer at pH 7.4, shows two sites (intercept =1.94) of equal affinity, each with an apparent dissociation constant of 6 ± 1 μM (A). Titration with MOPS causes changes in the chemical shift of signals from the PrP^{57-91} peptide (B), indicating a weak interaction with the peptide. The change in the chemical shift of the Histidine Hε1 signal of PrP^{57-91} is shown. To eliminate the possibility that pH effects were responsible for these changes the experiments were carried out in phosphate buffer at two different concentrations: 25 mM – open circles, and 50 mM – closed circles. The mode of copper binding observed in MOPS buffer gives a clear CD spectrum even at 1:1 stoichiometry (C). Spectra were recorded for an 11 μM sample of peptide in 50mM MOPS, 10 μM glycine, pH 7.4 with 1 copper (II) ion bound (1 eq $CuSO_4$ and 10 μM free copper bis-glycinate), and with 2 copper (II) ions bound (2 eq $CuSO_4$ and 100 μM free copper bis-glycinate). Addition of copper bis-glycinate to 300 μM produces no further change in the spectra, indicating that binding is saturated under these conditions at a stoichiometry of 2:1. The CD bands produced by the complexes formed in MOPS buffer are similar to those observed in the 4:1 complex formed in NEM buffer at pH 7.4.

Figure 6 Simulation of three mutually exclusive copper (II) binding modes in PrP^{57-91}

The concentrations of the main species present at equilibrium in simulations of competing modes of copper binding in PrP^{57-91} are shown over a range of total copper (II) concentrations. The simulations are described in detail in the text. They show that a single site of 3 nM affinity (mode A - $Cu^{A}P$) will predominate over four sites of 1 μM affinity (mode C - $Cu^{C}P$, $Cu^{C}{}_{2}P$, etc) only at low copper (II) concentrations. The concentrations of the $Cu^{B}P$ and $Cu^{C}P$ species did not exceed 1 μM at any point and are excluded for clarity. For illustration, an approximate predicted CD signal at 580 nM is shown, assuming that each copper (II) ion bound in modes B and C produces an equal signal at this wavelength and that ions bound in mode A produce no signal.

Figure 7 Equilbrium dialysis reveals two distinct forms of copper (II) coordination in PrP^{91-115}

Scatchard plots of equilibrium dialysis data for PrP^{91-115} show copper (II) binding with stoichiometries of 0.5:1 or 2:1, depending on the solution conditions. In 50 mM MOPS buffer at pH 7.4, with copper presented as a glycine complex, two sites (intercept =2.11) of equal affinity are observed, each with an apparent dissociation constant of 5.5 ± 0.5 μM (A). The formation of a 0.5:1 complex gives a non-linear Scatchard plot (B and C). The data were fitted numerically as described in the text, the results of which are represented as continuous lines. Dialysis against $CuSO_4$ in 5mM Tris, pH 7.4 (B), shows formation of a $Cu(PrP^{91-115})_2$ complex at low copper concentrations and a Cu_2PrP^{91-115} complex at higher copper concentrations. In 10 mM acetate, pH 5.5, only the $Cu\ (PrP^{91-115})_2$ complex is observed (C). CD spectra could be observed for both the $Cu(PrP^{91-115})_2$ and the Cu_2PrP^{91-115} complex (D). The spectra of the $Cu(PrP^{91-115})_2$ complex formed in 5 mM Tris, pH 7.4 is shown red (100 μM PrP^{91-115}, 60 μM $CuSO_4$ – i.e. 0.5 eq $CuSO_4$ and 10 μM free $CuSO_4$) and the $Cu(PrP^{91-115})_2$ complex formed in 10 mM acetate, pH 5.5 is shown in blue (100 μM PrP^{91-115}, 1 mM $CuSO_4$). The spectrum of the Cu_2PrP^{91-115} complex formed at pH 7.4 in 50mM MOPS is shown in purple (60 μM PrP^{91-115}, 200 μM copper bis-glycinate).

Figure 8 NMR of PrP^{91-115} copper (II) complexes

Formation of the $Cu(PrP^{91-115})_2$ complex can be observed by 1d ^{1}H NMR, with

broadening of the Hε1 signals of the two histidine residues indicating that they are both involved in copper coordination. Spectra are shown for a titration of 100 μM PrP^{91-115} with copper (II), in 5 mM Tris, pH 7.4, with the mole fraction of copper (II) added shown in the middle (A). The predicted fractions of free peptide (solid line) and peptide in the $Cu(PrP^{91-115})_2$ complex (dashed line), based on the equilibrium dialysis data, show that the $Cu(PrP^{91-115})_2$ is the dominant species below 1:1 stoichiometry (B). The integral of the histidine Hδ2 signal (open circles) is plotted relative to its starting value on the same axes.

Figure 9 Multiple modes of copper binding in PrP

(A) At least three different modes of copper (II) coordination occur within the octapeptide repeats at pH 7.4. The figure shows models for the structure of each mode of binding based on our data and that of others, alongside estimates for the dissociation constants. The cartoons represent the peptide backbone in the peptide PrP^{57-91}, with the histidine side chains shown as pentagons and the copper (II) ion represented by the black circle. **(B)** The figure shows the structure for the $Cu(PrP^{91-115})$ and $Cu_2(PrP^{91-115})$ complexes as described in the literature (left). At present there is insufficient data to propose a detailed structure for the $Cu(PrP^{91-115})_2$ complex, though our NMR data indicates that either two or three of the available histidines are involved in coordinating the metal ion (right). Estimates of the dissociation constants are given for all the complexes based on our measurements. The cartoons represent the peptide backbone and the sidechains of histidine 96 and 111. At present it is not possible to distinguish if either histidine is favored for any particular coordination position.

Figures

Figure 1

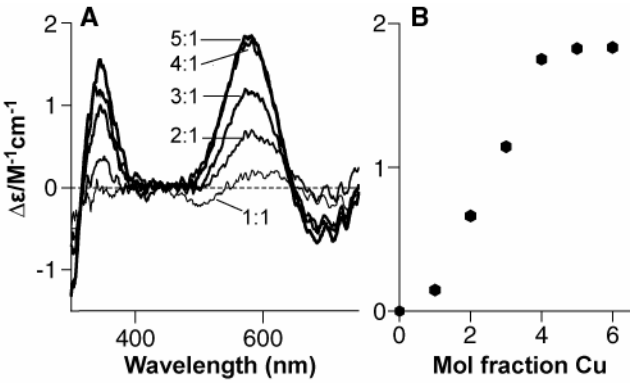

Figure 2

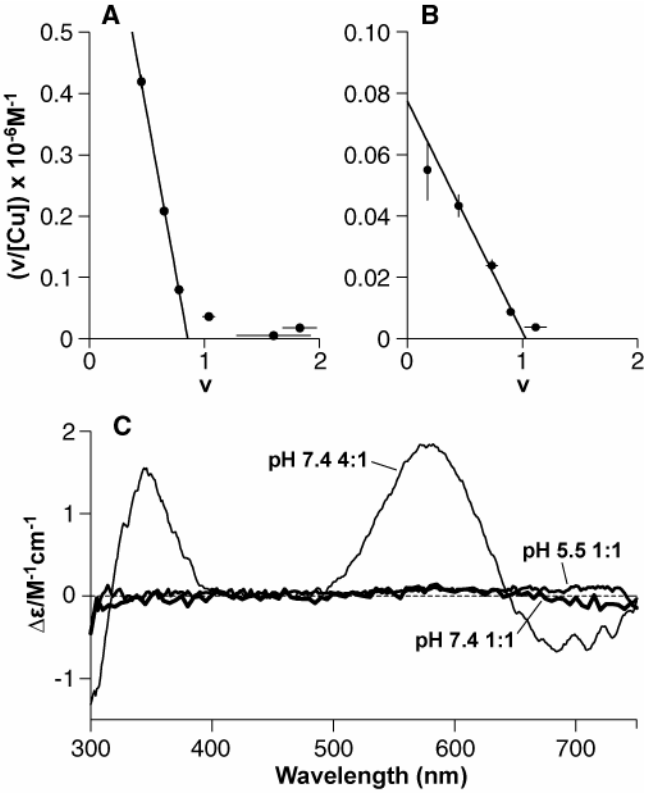

Figure 3

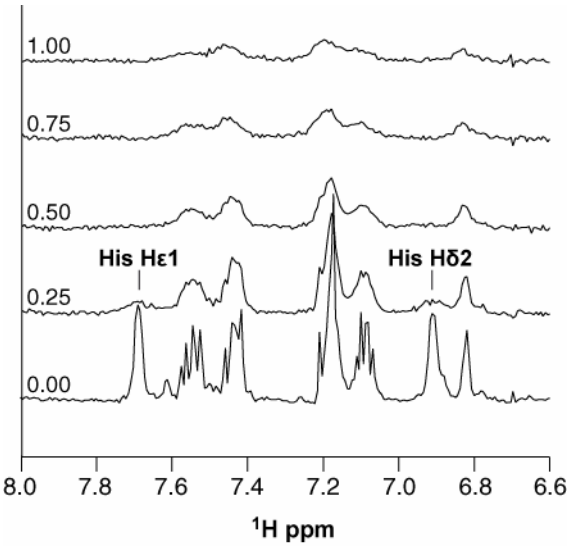

Figure 4

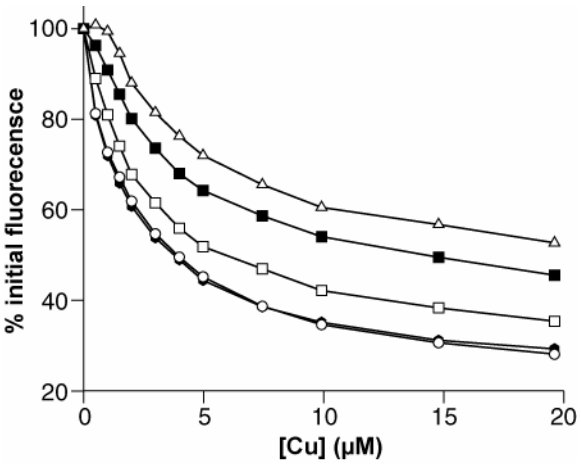

Figure 5

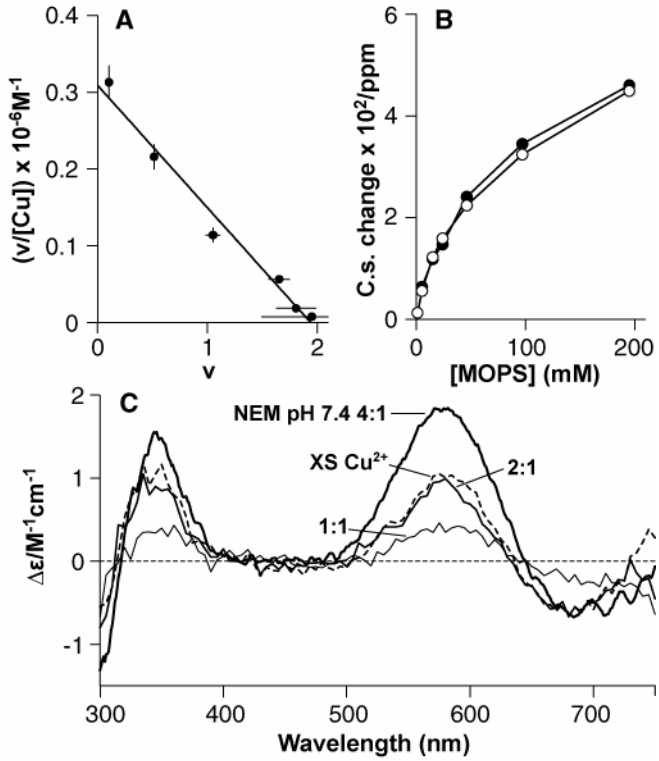

Figure 6

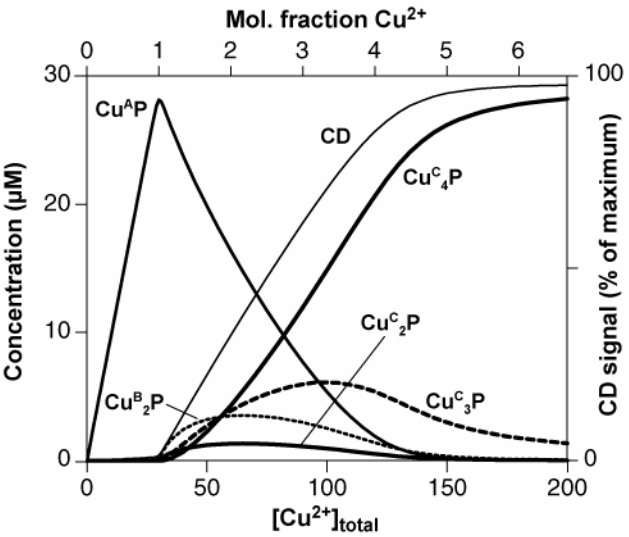

Figure 7

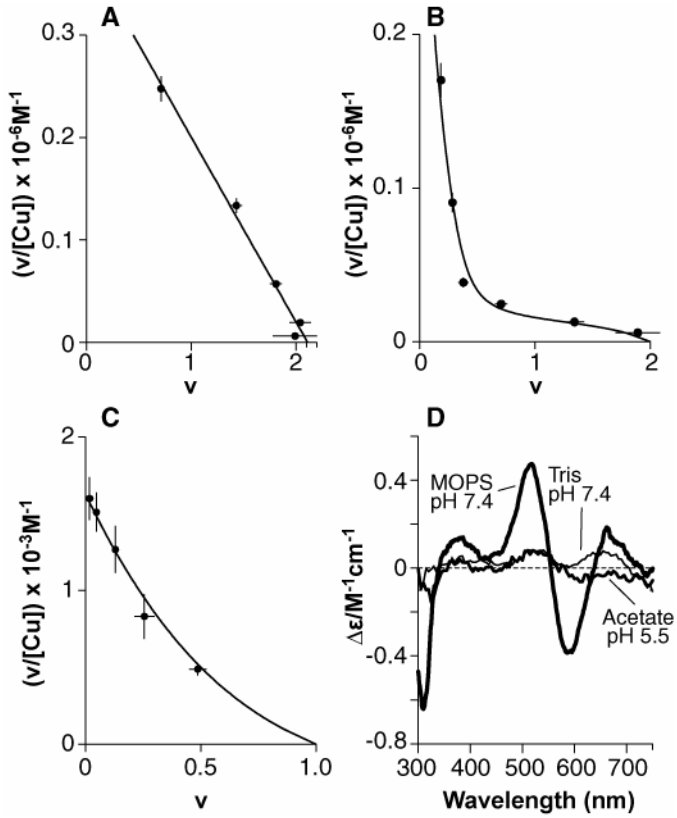

Figure 8

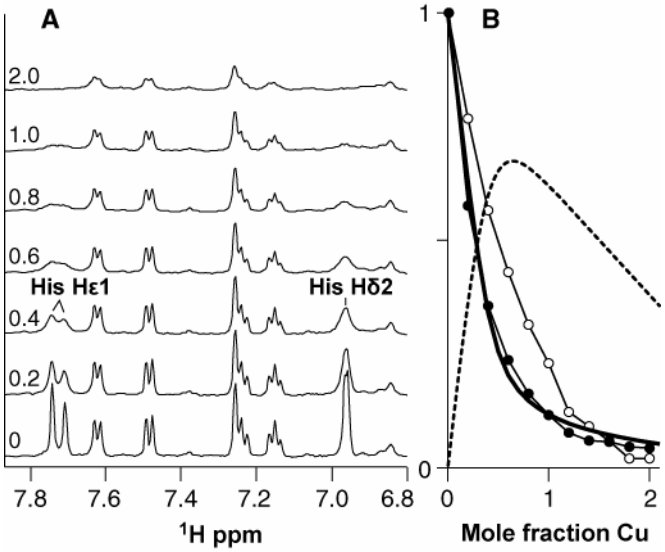

Figure 9